7.7. OXIDATION STATE IN CHONDRITES

ALAN E. RUBIN
University of California at Los Angeles

BRUCE FEGLEY
Massachusetts Institute of Technology

and

ROBIN BRETT
United States Geological Survey

The chemistry, mineralogy and oxidation state of planet-forming materials in the solar nebula were influenced strongly by the O fugacity (fO_2) of nebular gas. Information on fO_2 in the solar nebula may be preserved in relatively primitive samples that originally equilibrated with nebular gas and may not have been significantly altered by subsequent processes. Petrologic and chemical data can be used to arrange the major chondritic groups in order of decreasing degree of oxidation: CI > CM > CV > CO > LL > L > H > EL > EH. Many ungrouped chondrites as well as the silicate inclusions in IAB irons lie between H and E chondrites in this sequence. Refractory Ca,Al-rich inclusions (CAIs) in carbonaceous chondrites are depleted in Mo and W relative to other refractory siderophiles of similar volatility, consistent with oxidation of the refractory metals at high temperatures. Some Fremdlinge in CAIs contain V-rich magnetite and scheelite ($CaWO_4$) that apparently formed at higher fO_2 than other phases within the same inclusion. The enrichment and subsequent vaporization of silicate dust in certain regions of the solar nebula may have led to the locally high-fO_2 conditions required to have produced these Mo and W depletions and oxidized mineral assemblages. Oxygen-fugacity measurements can also be used to estimate the pressure at which meteorites cooled, thus
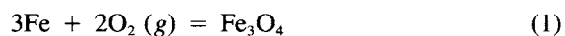
providing constraints on parent-body size. Such data indicate that chondrites were derived from parent bodies at least 30 to 70 km in diameter.

7.7.1. INTRODUCTION

The chondritic meteorites exhibit a large range of oxidation states, ranging from the FeO-poor enstatite chondrites to the magnetite- and water-bearing CI chondrites. In general, oxidation-state variations among chondrite groups are reflected in the oxidation state of chondrites' constituent Fe-Mg-Si-O-bearing minerals, principally olivine, pyroxene and metal. The oxidation state of this mineral assemblage reflects the O fugacity (fO_2) that prevailed during the final equilibration of the major ferromagnesian minerals with each other and with a gas phase. (The O fugacity is identical to the O partial pressure of an ideal gas.) Reactions exemplified by:

$$3Fe + 2O_2 \ (g) = Fe_3O_4 \tag{1}$$

$$2MgSiO_3 + 2Fe + O_2 \ (g) = Mg_2SiO_4 + Fe_2SiO_4 \tag{2}$$

and

$$Mg_2SiO_4 + 2FeSiO_3 = Fe_2SiO_4 + 2MgSiO_3 \tag{3}$$

which distribute Fe between metal, oxide and silicate phases, were presumably involved in this process. It is evident from Le Chatelier's Principle and from thermochemical data (see, e.g., Larimer 1968a) that, for objects of similar Fe content, the more-oxidized samples are characterized by higher concentrations of FeO in silicates and by the presence of magnetite (Fe_3O_4), whereas the less-oxidized samples are characterized by lower concentrations of FeO in silicates, the absence of magnetite and the presence of metallic Fe.

However, these considerations do not tell us where or how the observed oxidation states of the chondrites were established. One possibility is that the observed distribution of Fe between metal, oxide and silicate phases was originally established in the solar nebula by reactions between nebular gas and solid grains or liquid droplets and was unaltered by subsequent events. Another possibility is that the original oxidation states were altered and reset by gas-solid reactions associated with metamorphism and outgassing reactions on chondrite parent bodies. A third, more plausible, possibility is that a combination of nebular and parent-body processes have influenced to varying extents the oxidation states displayed by chondrites. In fact, the observed heterogeneity of the chondrites and the internal variation in oxidation states argue strongly for a mixture of nebular and planetary processes.

In this chapter we review the different oxidation-state indicators in chondrites and the methods used to estimate and infer O fugacities. Implications for the relative influences of nebular and parent-body processes are explored.

7.7.2. METHODS FOR MEASURING O FUGACITY

The intrinsic O fugacity of an equilibrium mineral assemblage is a function of both temperature and total pressure. Intrinsic fO_2 is related to the partial pressure of O in equilibrium with the mineral assemblage in a manner analogous to the way the activity of a component is related to concentration. Methods for measuring intrinsic fO_2 include:

1. The solid electrolyte-electrochemical method (Sato 1972). When properly done, this method is the most precise and accurate because the intrinsic fO_2 of the meteorite is measured directly as a function of temperature. Determinations of fO_2 in meteorites are listed (or referenced) in Brett and Sato (1984), Hewins and Ulmer (1984), Kozul et al. (1986) and the Basaltic Volcanism Study Project (1981).

2. Calculations based on mineralogical compositions determined by electron microprobe. As Eqs. (2) and (3) show, the proportion of oxidized Fe in mafic silicates reflects a meteorite's oxidation state. Such data, when combined with experimental and thermodynamic data, allow fO_2 to be calculated as a function of temperature. Calculations of fO_2 in ordinary chondrites based on olivine-metal-pyroxene equilibria (Williams 1971) are in good agreement with the determinations using the electrochemical method. Examples of such calculations are listed in Table 7.7.1.

3. Measurement of Ti^{3+}/Ti^{4+} in minerals using electron spin resonance (Live et al. 1986b). This method is useful for Ca,Al-rich inclusions (CAIs) that contain Ti-bearing minerals such as fassaitic pyroxene and

TABLE 7.7.1
**Types of Mineral Equilibria Used to Calculate fO_2 in Meteorites
as a Function of Temperature.**

| Equilibria	Reference
Fe-Ti oxide minerals	Harlow et al. (1982); McSween and Stolper (1978); Reid and Bunch (1975); Smith and Hervig (1979).
Phosphate-phosphide minerals	Olsen and Fuchs (1967); Olsen and Fredriksson (1966).
Pyroxene-metal-silica	Gooley and Moore (1976); Holmes and Arculus (1982).
Diopside-troilite-enstatite-metal-silica	Olsen and Fuchs (1967).
System Fe-Ca-Si-O-S	Larimer and Buseck (1974); Mueller and Saxena (1977).
System Fe-Si-O	Larimer (1968a).
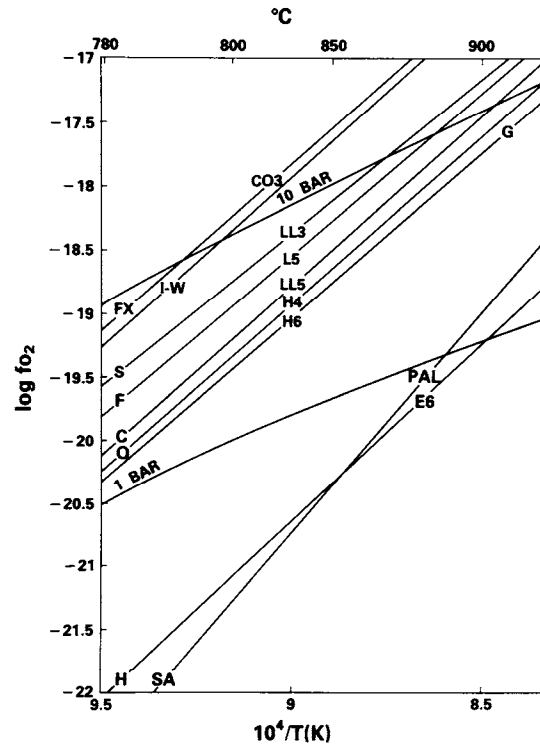
Fig. 7.7.1. Plot of linear regression relations for log fO_2 vs $1/T$ for several meteorites, with the iron-wüstite buffer shown for reference. The graphite surface is also shown at 1 bar and 10 bar pressure. Fx = Felix, S = Semarkona, F = Farmington, C = Cherokee Springs, O = Ochansk, G = Guarena, H = Hvittis, SA = Salta. Type of meteorite is also shown; PAL = pallasite.

hibonite. As in method (2), experimental and thermodynamic data are used to calculate fO_2.

4.   Phase equilibria methods in which the fO_2 of the synthetic assemblage is varied until the assemblage has the exact mineral composition of the meteorite at a given temperature (see, e.g., Stolper 1977). This method can be precise but is very time-consuming.

Figure 7.7.1 shows intrinsic fO_2 determinations of several meteorites (Brett and Sato 1984). Measurements of intrinsic fO_2 as a function of temperature of 2 little-metamorphosed chondrites, Semarkona (LL3) and Felix (CO3), show considerable scatter relative to five other chondrites of higher metamorphic grade. The bulk fO_2 of Semarkona and Felix decreased with time during the experiment. Brett and Sato interpreted these results to mean that the minerals constituting these meteorites formed over a range of fO_2

conditions and tended to equilibrate with each other during fO_2 measurement: the most oxidized minerals dominated the early fO_2 determinations and tended to equilibrate with other phases, causing a lowering of apparent fO_2 with time. The fact that meteorites of higher metamorphic grade do not exhibit this phenomenon suggests that equilibration with respect to fO_2 takes place between grades 3 and 4 of metamorphism. However, more experimental data are required to confirm this.

7.7.3. OXIDATION-STATE INDICATORS IN CHONDRITES

Intergroup Redox Variations

The clearest mineralogic indicator of the oxidation state of meteorite whole rocks is the occurrence of Fe in different oxidation states. Iron exists as a metal (Fe^0) alloyed with Ni and Co, as ferrous Fe (Fe^{2+}) in silicates, oxides and sulfides, and as ferric Fe (Fe^{3+}) primarily in oxides. As the oxidation state of a meteorite group increases, the proportion of oxidized Fe (e.g., FeO in silicates) increases at the expense of metallic Fe; similarly, because Fe oxidizes more readily than Ni or Co, metallic Fe-Ni becomes increasingly depleted in Fe and enriched in Ni and Co. These relationships are sometimes referred to as "Prior's rules" after G. T. Prior who studied chemical variations in meteorites in the early part of this century.

The variation in oxidation state among the ordinary chondrites is reflected by several mineralogical and chemical properties such as the compositions of olivine, pyroxene and kamacite, the bulk $FeO/(FeO + MgO)$ ratio and the bulk FeO/(total Fe) ratio. These properties indicate that, among ordinary chondrites, H chondrites are the most reduced, L chondrites are intermediate and LL chondrites are the most oxidized. In going from H to L to LL chondrites, the FeO contents of olivine and pyroxene increase, kamacite becomes richer in Co, and $FeO/(FeO + MgO)$ and FeO/(total Fe) both increase (Table 7.7.2). Figure 1.1.8 shows the variation in FeO content of olivine and pyroxene in the ordinary-chondrite groups; Fig. 7.4.2 illustrates the variation in kamacite and olivine compositions in ordinary chondrites. Magnetite is extremely rare to absent in H and L chondrites, but is present in several unequilibrated LL chondrites (e.g., Semarkona, Ngawi, Chainpur and Allan Hills A77278).

Carbonaceous chondrites are more oxidized than ordinary chondrites. CI chondrites are the most oxidized of all meteorites. They contain abundant H_2O, ~ 10 wt.% magnetite and no metal. CM chondrites have a somewhat lower oxidation state; they contain less H_2O and roughly 0.1 the amount of magnetite of CI chondrites. Some CM magnetite occurs in association with metal. CV chondrites comprise two subgroups; the oxidized subgroup, which includes Allende, averages ≤ 0.1 vol.% metal and ~ 2 vol.% magnetite; the reduced subgroup, which includes Leoville and Vigarano, averages 2 vol.% metal and considerably less magnetite (~ 0.3 vol.%) (McSween 1977a). CO

TABLE 7.7.2
Mean Compositional Properties of Ordinary-Chondrite Groups

	H	L	LL	ref[a]
Olivine (mol% Fa)	18.8	24.6	28.5	1
Low-Ca pyx (mol% Fs)	17.2	21.3	24.1	1
FeO/(FeO+MgO) (mol%)	17	22	27	2
Metallic Fe-Ni (mg/g)	168	77	~40	3
FeO/(total Fe)	0.38	0.66	0.88	4
Kamacite (mg/g Co)	4.4	8.9	~22	3,5
Bulk Fe (mg/g)	265	215	183	5
Bulk Ni (mg/g)	15.7	12.0	10.4	5
Kamacite/taenite	~5	~1	~0.4	3

[a]References: (1) Gomes and Keil (1980); (2) Wasson (1985); (3) Afiattalab and Wasson (1980); (4) E. Jarosewich, unpublished data; (5) G. W. Kallemeyn, unpublished data (1987).

chondrites average 2.5 wt.% metal (McSween 1977b) and contain only minor magnetite (primarily inside chondrules).

At the opposite extreme are the highly reduced enstatite chondrites. The EH (high-Fe) group averages 22 wt.% metallic Fe-Ni. Very little FeO occurs in the silicates: pyroxene contains < 1 mol% $FeSiO_3$ (i.e., Fs < 1). EL chondrites contain about the same amount of metal, but even less FeO in the pyroxene. Both groups are so reduced that metallic Si is dissolved in the kamacite. EH kamacite averages ~ 3 wt.% Si, whereas EL kamacite averages only one-third as much. Magnetite is absent from both groups.

The presence of highly reduced refractory minerals (e.g., oldhamite, CaS; osbornite, TiN; sinoite, Si_2N_2O) in enstatite chondrites is in accord with the above observations. Experimental data on CaS stability (Larimer 1968b) and theoretical calculations of mineral stabilities under low O fugacities (Larimer and Bartholomay 1979) show that these accessory minerals are only stable under highly reducing conditions comparable to those required for formation of essentially FeO-free silicates and Si-bearing metal.

From petrologic data, all of the major chondrite groups can be arranged in order of oxidation state. From highest to lowest, they are: CI > CM > CV > CO > LL > L > H > EL > EH. The relative positions of EL and EH are uncertain. Bulk compositional data are consistent with this ordering: the atomic ratio of oxidized Fe to Si decreases from CI to E chondrites. This is illustrated in Fig. 7.4.1; for the present discussion, we need only consider the projection of the points onto the abscissa of that diagram. The mean FeO_x/Si ratio of each chondrite group falls on the abscissa in the same order of oxidation state as that derived above from petrological considerations.

The silicate inclusions in IAB irons are approximately chondritic in bulk composition and can be added to the list. IAB pyroxene (Fs 4–8) is low in FeO, indicating that these inclusions are intermediate in oxidation state be-

tween H and E chondrites. Three closely related meteorites, Winona, Mount Morris (Wisconsin) and Pontlyfni are similar in oxidation state and bulk and O-isotopic compositions to IAB silicates; they probably belong to group IAB (Kallemeyn and Wasson 1985). Certain other ungrouped meteorites are also intermediate in oxidation state between ordinary and enstatite chondrites; they include Kakangari, Suwahib Buwah, Acapulco, Allan Hills A77081, Willaroy and the chondrule-bearing silicates in the Netschaëvo IIE iron.

The ordering of chondrite groups by oxidation state is based principally on the nature of interchondrule material, some of which, e.g., magnetite in CI and CM chondrites, probably formed by secondary alteration. If we restrict our attention to chondrules (which are nebular products; see Chapter 9.3), a more muddled sequence emerges. Chondrules with reduced (i.e., FeO-poor) olivine and pyroxene phenocrysts constitute 100% of the chondrules in EH chondrites, $\geq 90\%$ of those in CV, CM and CO chondrites, and only 50 to 90% of those in ordinary chondrites (Table 9.1.1). The reason for these differences is unclear.

Although chondrite groups vary in overall oxidation state, individual chondrites of petrographic types 2 and 3 are highly disequilibrated assemblages that can preserve materials formed under different fO_2 conditions. For example, Si- and Cr-bearing metallic Fe-Ni grains occur in CM2 (e.g., Murchison), CO3 (e.g., Allan Hills A77307), LL3 (e.g., Bishunpur) and EH3 (e.g., Qingzhen) chondrites. These grains are probably relicts of high-temperature, low-fO_2 conditions in the early solar nebula. They must have been prevented from oxidizing (via reaction with H_2O), possibly because they were encapsulated in larger silicate grains (see, e.g., Rambaldi et al. 1980).

Intragroup Redox Variations in Ordinary Chondrites

Individual equilibrated chondrites within a single chondrite group can also have different oxidation states. Because diffusion in olivine is relatively rapid, olivine compositions are a useful indicator of oxidation state. Figure 7.7.2 shows the distributions of Fa in olivines from 10 H-group chondrites (8 of which are from China). The distribution in each chondrite is narrow; σ_{Fa} ranges from 0.3 mol% in Dhajala, Changxing and Lunan to 0.9 mol% in Changde. Although Dhajala (type 3.8) has sharply delineated chondrules with glassy-to-cryptocrystalline mesostases, its olivine is rather uniform. In contrast, low-Ca pyroxene in Dhajala is heterogeneous (see Fig. 1 of Noonan et al. 1976). A few olivine grains in Anlong, Changde, Enshi and Xingyang are obviously not in equilibrium with the majority. Scott et al. (1985) found that at least 25% (and probably most) type 4 to 6 ordinary chondrites contain rare olivine and/or pyroxene grains with Fe/(Fe + Mg) ratios that differ significantly from the majority. Such chondrites are probably breccias that were assembled after individual components were equilibrated during metamorphism.

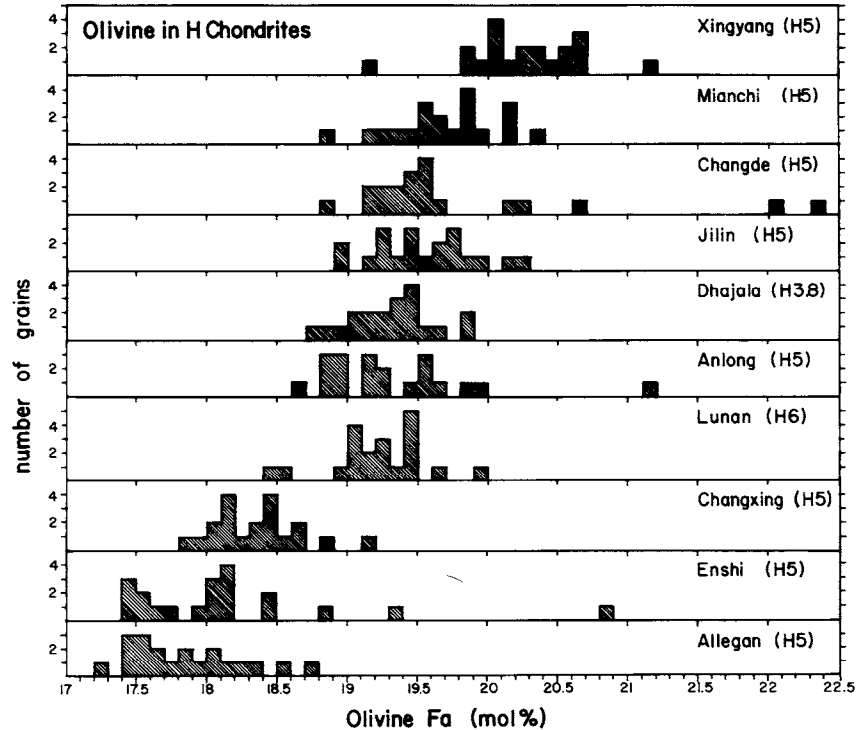Several of the 10 chondrites (e.g., Allegan, Lunan and Xingyang) have

Fig. 7.7.2. Compositional distributions of 20 olivine grains in 10 H-group chondrites. The narrow distributions result from equilibrium at specific oxidation states; i.e., the oxidation state of Xingyang is considerably higher than that of Allegan. The occurrence of a few olivine grains with aberrant compositions suggests that several of these chondrites may be breccias that formed after metamorphic equilibration.

mean olivine compositions that differ significantly from one another. These chondrites are not in equilibrium with each other and must have been derived from different metamorphic terranes on the H parent body or bodies. It is unclear whether the material in each terrane preserved oxidation states acquired in the nebula during agglomeration or whether local parent-body processes affected terranes differently. In the latter case, reducing agents such as graphite could have been responsible. However, Scott et al. (1986) found that mean FeO contents of olivine and low-Ca pyroxene in ordinary chondrites increase by 3 to 5% from type 4 to 6 and attributed these properties to nebular and accretionary processes.

7.7.4. INFERENCES ABOUT SOLAR-NEBULAR PROCESSES

The available data on chondrite oxidation states and intrinsic O fugacities can be interpreted in terms of nebular processes, parent-body processes

or a combination of both. It is reasonable to expect that relatively unaltered primitive samples that originally equilibrated with nebular gas and still retain the imprint of nebular processes preserve information about nebular O fugacity variations and fO_2 values. Similarly, it is reasonable to expect that metamorphosed meteorites may help constrain parent-body processes. These two propositions are useful operating assumptions which we employ in our discussion in this section and the following one.

Before trying to interpret the oxidation state of relatively unaltered primitive chondrites and their components in terms of a solar-nebular origin, we need to know how the fO_2 of nebular gas was regulated and what the expected oxidation states are of solid materials that equilibrated with the gas.

The fO_2 of an H_2-rich gas with relative solar atomic proportions of $H(1350):O(1):C(0.6)$ is controlled by the reaction:

$$H_2 + 0.5\ O_2 = H_2O. \tag{4}$$

The equilibrium fO_2 for Reaction (4) is given by the expression:

$$\log_{10} fO_2 = 2\log_{10}(H_2O/H_2) + 5.59 - 25,598/T \tag{5}$$

which utilizes the latest JANAF (1986) data and is valid from 300 to 2500 K. For reference, the (H_2O/H_2) number ratio for solar-composition gas is $\sim 5 \times 10^{-4}$ (because all C is present as CO) and the fO_2 at 1600 K is $\sim 10^{-17}$ bar (independent of total pressure in the P,T region where CO is the dominant C-bearing gas).

It is clear from the relative abundances of C and O that the (H_2O/H_2) ratio in gas of solar composition is also affected by equilibria between oxidized and reduced C-bearing gases (but not by graphite formation which cannot occur at temperatures > 470 K or pressures $> 10^{-7.6}$ bar at equilibrium in a gas of solar composition [Lewis et al. 1979]). These equilibria are exemplified by the reaction:

$$CO + 3H_2 = CH_4 + H_2O \tag{6}$$
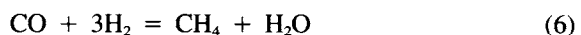
which shifts to the right with decreasing temperature at constant pressure. Thermodynamic calculations (see, e.g., Prinn and Fegley 1988) show that the destruction of CO (which is the major C-bearing gas at high temperatures) by Reaction (6) is 50% complete at ~ 710 K (10^{-3} bar total pressure) or at ~ 520 K (10^{-6} bar total pressure). If thermochemical equilibrium is maintained, the complete conversion of CO to CH_4 ultimately increases the (H_2O/H_2) ratio to $\sim 1 \times 10^{-3}$.

However, the kinetics of the CO to CH_4 conversion are sufficiently slow (relative to the rates of nebular radial mixing or thermal evolution) so that Reaction (6) probably did not go to completion at low temperatures (Lewis

and Prinn 1980). In fact, the CO to CH_4 conversion is quenched at such a high temperature that essentially all C is present as CO; CH_4 does not form (Prinn and Fegley 1988).

The oxidation state of FeO-bearing silicates in equilibrium with solar-nebular gas and metallic Fe can be calculated using experimental and thermodynamic data for Reactions (2) and (4). If we assume ideal solution for Fe and Mg in olivine, the data of Larimer (1968a) yield the expression:

$$\log_{10} X_{Fa} = \log_{10} (H_2O/H_2) - 0.74 + 1690/T \qquad (7)$$

which relates the mole fraction of fayalite in olivine coexisting with metallic Fe to the (H_2O/H_2) ratio and temperature of the coexisting gas phase.

An important implication of Eq. (7) is that olivines that equilibrated with solar-composition gas ($H_2O/H_2 \simeq 5 \times 10^{-4}$) at high temperatures will be FeO-poor while olivines that continued to equilibrate with the gas phase down to low temperatures will be FeO-rich. For example, the calculated fayalite content of olivine in equilibrium with solar-composition gas at 1000 K is only ~ 0.4 mol%, but is much larger (~ 22 mol%) at 500 K. It is evident from experimental and thermodynamic data on the exchange reaction (Eq. 3) that similar FeO enrichments are also expected in low-Ca pyroxenes at low temperatures.

We can use this basic background to evaluate different models for the origin of the olivines found in primitive, little-metamorphosed chondrites. These olivines have heterogeneous compositions that vary from Fa 0.3 to Fa > 90 mol% in type-3 ordinary chondrites (e.g., Semarkona), CO3 chondrites (e.g., Colony) and CM2 chondrites (e.g., Mighei). The high-fayalite olivines occur primarily in fine-grained matrix material, and, in some cases, in matrix-like rims around metal grains (see, e.g., Scott et al. 1984; Chapter 10.2). For present purposes, these fayalitic olivines are potentially the most interesting, and we will concentrate on them. (The origin of coarser-grained olivine in the same meteorites is discussed in Chapter 10.4.)

The simplest model for explaining the origin of such fayalite-rich olivines (Fa $\simeq 60-90$) is equilibration with solar-composition gas at low temperatures. Taken at face value, Eq. (7) indicates that temperatures of ~ 420 to 440 K are required to produce olivines with 60 to 90 mol% fayalite. Although this model is qualitatively appealing, it implicitly assumes intimate contact and complete equilibration of three different solids (metallic Fe, low-Ca pyroxene and olivine) down to temperatures of ≤ 500 K. This is questionable, especially in light of the slow rate of solid-state diffusion at these low temperatures.

An alternative model involves the melting and rapid cooling of highly oxidized precursor materials, as in, for example, the formation of chondrules. In this scenario, which has been recently revived by Wood (1985), different degrees of partial equilibration of rapidly cooling olivines with nebular gas,

assumed to have a solar (H_2O/H_2) ratio, are reflected in the observed heterogeneity of olivine compositions. However, in some cases surviving relict grains in chondrules are more reduced than adjacent chondrule phenocrysts (Wood 1988). Furthermore, if chondrules were formed from oxidized (FeO-rich) precursors, they must have lost considerable amounts of metal during melting and reduction because, in general, chondrules are metal poor. For example, the average Fe/Mg ratio of chondrules in Semarkona (LL3) is only 40% of that of the whole rock. The paucity of metallic spherules relative to chondrules in chondrites suggests that most chondrules probably did not form from highly oxidized precursors.

Grossman and Wasson (1983a,b) proposed a third possible model in which the observed olivine heterogeneity is ascribed, at least in part, to variations in the grain sizes of nebular condensates. They proposed that, with decreasing temperature, finer-grained materials (with higher-surface/volume ratios) were preferentially enriched in FeO relative to coarser-grained materials (with smaller surface/volume ratios). Thus, this model attempts to remedy the kinetic inhibition of low-temperature gas-solid and solid-solid reactions by postulating grain sizes that were small enough to permit equilibration. One potential pitfall to this model is that agglomeration of fine grains may have produced coarser, chemically unreactive grains faster than FeO incorporation could proceed.

However, another alternative model may not suffer from such kinetic constraints. Examination of Eq. (7) shows that high-fayalite olivines could be formed at high temperatures (where reactions between gas and solids proceed much faster) under more oxidizing conditions. For example, an increase in the (H_2O/H_2) ratio from the canonical solar value of $\sim 5 \times 10^{-4}$ to a much higher value of $\sim 10^{-1}$ increases the fayalite content of olivine from ~ 0.1 mol% to ~ 29 mol% at 1400 K; more detailed calculations by Palme and Fegley (1987) confirm this general result. The formation of fayalitic olivines by high-temperature oxidation is both theoretically plausible (Palme and Fegley 1987) and consistent with observational data (Nagahara 1984; Hua et al. 1987); it is also consistent with the high-temperature oxidation of refractory mineral assemblages such as the CAIs found in carbonaceous chondrites. (See Chapter 10.3 for detailed discussion of CAIs.)

Several research groups have proposed that CAIs actually contain evidence for oxidizing conditions in the solar nebula. These proposed indicators are summarized in Table 7.7.3, which also shows whether or not these indicators of high-temperature oxidation are potentially reversible (i.e., if they can be reset by either more or less oxidizing conditions). The concept of reversibility is important because the different indicators may be recording fO_2 values that are characteristic of separate events.

The most common evidence in CAIs for oxidizing conditions in the solar nebula involves depletions of Mo and W (both of which are readily oxidized) relative to other refractory siderophiles of similar volatility that are far less

TABLE 7.7.3
Proposed Oxygen-Fugacity Indicators in Ca,Al-Rich Inclusions
in Carbonaceous Chondrites

| Proposed Indicator	Reversible?	Ref.[a]
Barium depletions	No	1
Cerium depletions	No	1–3
Color of hibonite	Yes	4
Fremdlinge minerals (e.g., scheelite)	No	5,6
Refractory metal (Mo, W) depletions	No	7
Siderophile behavior of Hf, Nb, Ta, Zr	No	8
(Ti^{3+}/Ti^{4+}) ratios in hibonite	Yes	9,10
(Ti^{3+}/Ti^{4+}) ratios in Ti-bearing pyroxenes	No	11
Uranium depletions	No	1
Vanadium depletions	No	1

[a]References: (1) Davis et al. (1982); (2) Boynton (1984); (3) Fegley (1986); (4) Ihinger and Stolper (1986); (5) Armstrong et al. (1985a); (6) Bischoff and Palme (1987); (7) Fegley and Palme (1985); (8) Fegley and Kornacki (1984); (9) Live et al. (1986b); (10) Live et al. (1986a); (11) Beckett (1986).

readily oxidized (Re, Os, Ir, Ru and Pt). In fact, 77% of all CAIs (20/26) for which INAA data of the 7 refractory metals are available (H. Palme and B. Spettel, personal communication, 1986) show Mo depletions at the 95% confidence level; 15% show W depletions at the 95% confidence level. These statistics are consistent with the production of Mo depletions at lower fO_2 than W depletions (Fig. 7.7.3).

The refractory-metal abundance patterns displayed in Fig. 7.7.3 are the result of an interplay between the vapor pressures of Mo and W and the tendency of these two metals to be oxidized in the gas phase by reactions such as:

$$Mo + H_2O = MoO + H_2 \qquad (8)$$

and

$$W + H_2O = WO + H_2. \qquad (9)$$
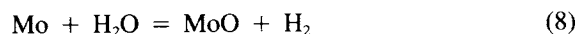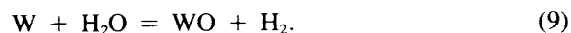
Fegley and Palme (1985) discussed these factors in detail and showed that the characteristic nature of the Mo- and W-depletion patterns can be produced only by oxidation at high temperatures. In particular, the observed depletions do not correlate with the degree of CAI alteration and are not unique to Allende but are observed in 6 of 7 carbonaceous chondrites (Allende, Arch, Efremovka, Grosnaja, Leoville and Ornans but not Essebi) from which CAIs have been analyzed. Fegley and Palme (1985) showed that, at an assumed total pressure of 10^{-3} bar, the (H_2O/H_2) ratios indicated by the Mo and W depletions in CAIs range from slightly larger than the solar value ($\sim 5 \times 10^{-4}$) to about 10^{-1}. Figure 7.7.4 illustrates a highly fractionated metal pattern observed
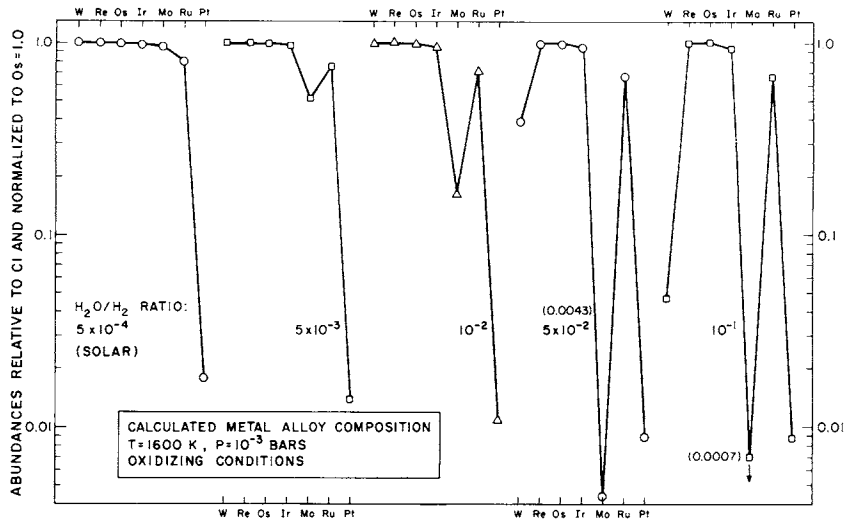
Fig. 7.7.3. Mo and W depletions in refractory metal alloys as a function of O fugacity at constant temperature and pressure. The O fugacity is expressed as the (H_2O/H_2) ratio, and can be calculated from $\log_{10}K$ (H_2O, g) using Eq. (5).
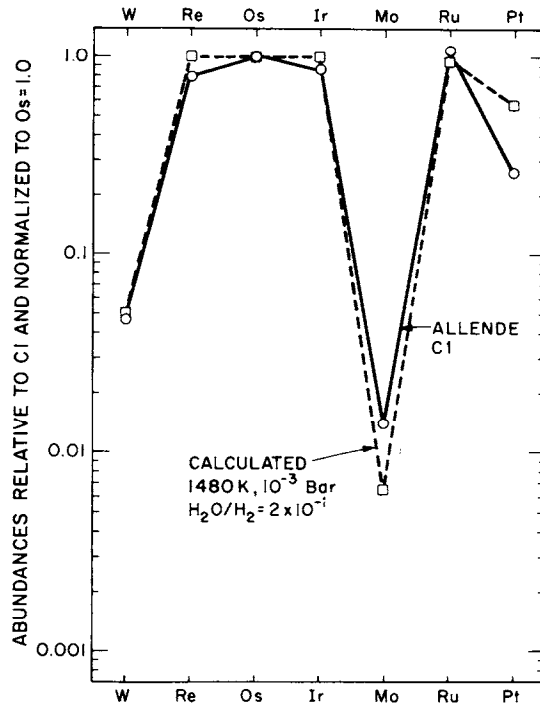

Fig. 7.7.4. Observed and calculated refractory-metal abundances in Allende FUN inclusion C1. The observed composition is from EDS/SEM analyses of metal grains by D. A. Wark.

in the Allende FUN inclusion C1 and a calculated match to it. (FUN inclusions are discussed in detail in Chapter 14.3.) Such highly fractionated patterns were found to be typical of equilibration at (H_2O/H_2) ratios of $\sim 10^{-1}$ and not limited to FUN inclusions.

Similar (H_2O/H_2) ratios in the range of 10^{-2} to 10^{-1} for equilibration of hibonite from the Allende Blue Angel inclusion with nebular gas were suggested by Ihinger and Stolper (1986). They had proposed earlier that the color of hibonite (ideally $CaAl_{12}O_{19}$ but, in many cases, containing Ti, V, Fe, Mg, Si and Cr in coupled substitutions) could be used as an O-fugacity indicator in CAIs. Related work by Live et al. (1986a) suggested that the Ti^{3+}/Ti^{4+} ratio in meteoritic hibonites could be used as an fO_2 indicator. Results for the spinel-hibonite inclusion SH-7 give an upper limit on fO_2 that is 10^3 to 10^4 times more oxidizing than solar gas. This upper limit is comparable to the fO_2 values estimated from Blue Angel hibonite and from the Mo and W depletions in CAIs.

Thus, high-temperature oxidation in the solar nebula is indicated by the fayalitic olivines found in primitive, little-metamorphosed chondrites and by several features of CAI trace-element chemistry and mineralogy. However, no completely satisfactory mechanisms have been proposed to account for such large implied fO_2 variations in the solar nebula. Several of the most popular (although not necessarily correct) suggestions are reviewed below.

One frequently proposed mechanism for attaining high fO_2 in the nebula is by the enhancement of the ratio of silicate-dust to gas. Simple mass-balance arguments illustrate why this mechanism is popular. Approximately 20% of all O resides in anhydrous silicate dust (taken as MgO + SiO_2 + FeO + CaO + Al_2O_3), $\sim 20\%$ is in $H_2O(g)$, and the remaining $\sim 60\%$ is in $CO(g)$. This latter O is essentially locked up in the gaseous CO, which is thermodynamically stable at high temperatures and kinetically stable against conversion to CH_4 at low temperatures (Lewis and Prinn 1980).

Table 7.7.4 shows the effects of silicate-dust enrichments on O fugacity in the solar nebula where the O fugacity at any temperature can be calculated from the tabulated (H_2O/H_2) ratio using Eq. (7). In order for the dust to affect fO_2, it must first be vaporized. Dust enrichments of 50 to 500 times greater than solar are required to produce (H_2O/H_2) ratios corresponding to the observed fayalite compositions in olivines in primitive chondrites (Nagahara 1984; Palme and Fegley 1987; Hua et al. 1987), the observed Mo and W depletions in CAIs (Fegley and Palme 1985) and the observed colors of meteoritic hibonites (Ihinger and Stolper 1986). Because approximately equal amounts of O are present in silicate dust and in water, the required enrichment factors for ice-plus-dust mixtures are about a factor of 2 smaller than the dust-enrichment factors unless ice and dust are present in grossly nonsolar proportions. Dust enrichment could conceivably occur at the nebular midplane due to gravitational settling and collisions or at the boundary of the nebular surface with interstellar space due to infalling parcels of interstellar grains.

TABLE 7.7.4

Effects of Dust Enrichments on (H_2O/H_2) Ratios in the Solar Nebula[a]

Dust Enrichment	X^b Dust	Mass % Dust	H_2O/H_2^c
1 (Solar)	2.0×10^{-4}	0.5	5×10^{-4}
50	0.01	20	1.6×10^{-2}
250	0.05	55	7.6×10^{-2}
500	0.09	71	0.15
750	0.13	78	0.23
1000	0.16	83	0.30
10^4	0.67	98	3.0^d
10^5	0.95	99.8	30
10^6	0.993	99.98	300

[a] Dust = $MgO + SiO_2 + FeO + CaO + Al_2O_3$.
[b] X = mol fraction = (mol dust)/(mol dust + gas).
[c] Excludes the ~60% of O present in $CO(g)$ which is thermodynamically stable at high T and kinetically stable against conversion to CH_4 at low T.
[d] At dust enrichments of ≥ 3200, H_2O becomes the dominant H reservoir. Calculations presented for higher enrichments assume an infinite H supply.

Dust enrichment has several other consequences in addition to increasing the O fugacity. These include increases in the opacity, viscosity and coagulation rate in the dust-enriched region of the nebula. This mechanism also requires that (1) a powerful but, as yet, unidentified heat source capable of vaporizing at least the MgO- and SiO_2-bearing phases in the dust be operative after dust enrichment has occurred, and (2) the total amount of dust is only partially vaporized so as to maintain high opacity and slow cooling rates. Furthermore, extreme dust-to-gas fractionations are required to generate the large fO_2 values that may be required at high temperatures to produce some of the oxidized phases such as scheelite ($CaWO_4$) and magnetite which are observed in Fremdlinge (Armstrong et al. 1985a; El Goresy et al. 1978; Bischoff and Palme 1987). In addition, the presence of the low-temperature phases observed in Fremdlinge such as Ge-bearing alloys and sulfides (see, e.g., Armstrong et al. 1985b; El Goresy et al. 1978) is a potential problem unless they were incorporated into the Fremdlinge after the high-temperature oxidizing event, possibly during a second oxidizing event at low temperatures.

7.7.5. INFERENCES ABOUT PARENT-BODY PROCESSES

Pressure and Depth of Origin of Meteorites

The irons, mesosiderites, achondrites and ordinary chondrites all probably had fO_2 values of the graphite surface (i.e., the fO_2 value that is in equilibrium with an equilibrium assemblage of C, CO and CO_2) at the pressures at which these meteorites cooled (Brett and Sato 1984). Oxygen-

fugacity measurements of these meteorites can provide information on the pressures at which they cooled and hence provide constraints on parent-body size. The pressures obtained seem reasonable; those for chondrites are consistent with the results of Pellas and Storzer (1981) who used the independent method of fission-track thermometry. Nevertheless, the fO_2 method of pressure determination must receive further confirmation before it can be fully accepted.

The fO_2 of mixtures of CO, CO_2 and graphite is remarkably sensitive to pressure (especially at geologically low pressures), whereas the fO_2 of other condensed species (such as Fe-bearing silicates) and gas is relatively insensitive to pressure. Sato (1978) refined the log fO_2 vs $1/T$ plots at various pressures for equilibria involving $C-CO-CO_2$, taking into account the nonideal behavior of the gases involved (Fig. 7.7.5). If a meteorite contains no graphite, $CO-CO_2-C$ equilibria have no relevance. If graphite is not the C-bearing solid phase, then the activity of C will be less than unity, and the fO_2 of this phase with CO + CO_2 will be somewhat higher than that for equilibria in-
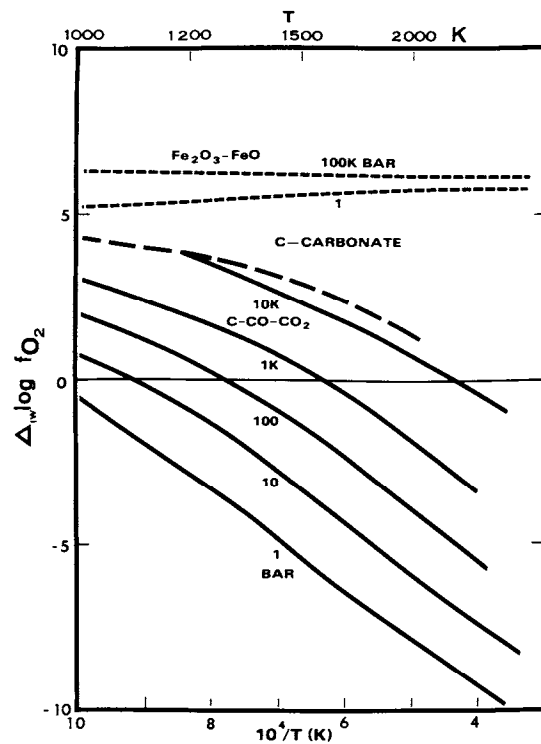

Fig. 7.7.5. Isobars in the graphite-CO-CO$_2$ system as a function of T and Δ_{Iw} log fO_2. The latter function is log fO_2 of the graphite surface minus log fO_2 of IW. Equilibria involving carbonate dominate at higher pressures, as shown (figure after Brett and Sato 1984). IW = iron-wüstite.

volving graphite at a given T and P. If a meteorite contains graphite and shows no evidence of reduction, then it lay at or below the fO_2 at which graphite is stable with CO + CO_2 (Fig. 7.7.5; see also Fig. 4 of Sato 1979). By measuring the fO_2 in equilibrium with the meteorite at a given temperature at low pressure, it is possible to arrive at a minimum pressure for equilibration of the meteorite at that temperature (the pressure for C-CO-CO_2 equilibrium—i.e., the graphite surface—corresponding to the fO_2 and T). However, if the meteorite was undergoing reduction at the given temperature, then it lay on the graphite surface, and the precise pressure can be determined if the fO_2 at the temperature is known.

Enstatite Chondrites

Because enstatite chondrites were probably not reduced by graphite during metamorphism, they most likely lay beneath the graphite surface. Inspection of Fig. 7.7.1 indicates that if enstatite chondrites were reduced, the pressure must have been ≤ 1 bar. This is in accord with their proposed reduction in the solar nebula (Larimer and Bartholomay 1979).

Iron Meteorites

Calculations by Olsen and Fuchs (1967), based on phosphate-phosphide equilibria, suggest that the fO_2 values of iron meteorites lie within the range of ordinary chondrites. Prinz et al. (1983) reported that some iron meteorites appear to have been reduced by C; fO_2 measurements or calculations should be made on these meteorites, because applying the calculations of Olsen and Fuchs (1967) to Fig. 7.7.5 suggests a pressure of only a few bars. However, such meteorites may not have been reduced.

Mesosiderites

Thermodynamic calculations by Harlow et al. (1982) based on Fe-Ti-O equilibria indicate that the fO_2 of mesosiderites lies in the upper range of that of chondrites. Agosto et al. (1980) suggested that some mesosiderites were reduced by C or P. If it was C, then inspection of Fig. 7.7.5 indicates that mesosiderites formed at a pressure of about 20 bar. If reaction by C did not occur, then this pressure is a minimum. Snellenburg et al. (1979) deduced log fO_2 of $- 20$ at $840°$ C for 4 mesosiderites of low metamorphic grade. This corresponds to pressures of a few bars.

Achondrites

Oxygen-fugacity data on achondrites provide little information on pressure during cooling. Brett et al. (1977) deduced a minimum pressure during cooling of 50 to 80 bar for the unique achondrite, Angra dos Reis. This corresponds to a depth of 6 to 10 km in a parent body 250 km in diameter having a specific gravity of 3.5 and to a depth of 1000 to 1600 m in a lunar-sized body.

Ordinary Chondrites

Larimer (1968a) suggested that metamorphism of chondrites essentially took place in a closed system. He pointed out, however, that metallic Fe decreases slightly with percent-mean-deviation of Fa in olivine within individual chondrite groups; this suggests that some reduction occurred during metamorphism. Dodd (1974) showed that metal in H3 chondrites tends to contain more Ni than that in H4–6 chondrites. When coupled with the fact that C in ordinary chondrites decreases with increasing metamorphic grade (see, e.g., Mason 1979), this observation suggests that a small amount of reduction by C took place in ordinary chondrites during metamorphism. The reaction probably did not go to completion during metamorphism because C dissolved in the metal, lowering its activity.

The fact that some reduction by C appears to have taken place, suggests that the ordinary chondrites lay at or close to the graphite surface during their metamorphic histories. Inspection of Fig. 7.7.5 indicates that the graphite surface within the T-fO_2 range of ordinary chondrites is at a pressure of about 3 to 5 bar at 800° C, and about 8 to 20 bar at 900° C. The valid temperature to use for the pressure estimate is the one at which graphite ceased to equilibrate with the meteorite (probably closer to 900° C). Thus, the chondrites were probably at pressures of 3 to 20 bar. The *minimum* parent body (having a specific gravity of 3.5) required is 30 to 70 km in diameter.

Range of Parent-Body Redox Conditions

Carbon is almost ubiquitous in meteorites. A range of redox conditions as a function of temperature and depth is a natural consequence of the buffering effect of the graphite surface in a parent body (Fig. 7.7.5). Increasing depth (pressure) within the parent body favors higher fO_2, as does increasing temperature. However, the effect of pressure on iron-wüstite (IW) and Fe^{2+}/Fe^{3+} reactions is negligible; the fO_2 of these boundaries increases more steeply than that of the graphite surface as a function of temperature (Fig. 7.7.5). (The IW buffer is the fO_2 value that is in equilibrium with metallic Fe and wüstite ($Fe_{1-x}O$) as a function of temperature.) A parent body that was heated sufficiently to cause equilibration with respect to fO_2 would have a redox state in its interior that reflected the T/P gradient. A steep T/P gradient would produce a thin reduced surface layer, an oxidized near-surface layer and an interior that was increasingly more reduced with depth (Fig. 7.7.6).

The final oxidation state of the body depends on the T/P gradient at the temperature at which equilibration ceased during cooling. If equilibration was not achieved due to insufficient temperature, or insufficient time of metamorphism, unequilibrated meteorites would have resulted. The situation would have become complicated if all the graphite was consumed, in which case, one of the various buffers involving Fe species would have taken over. If metallic Fe-Ni was present, C would have dissolved in it. When all graphite
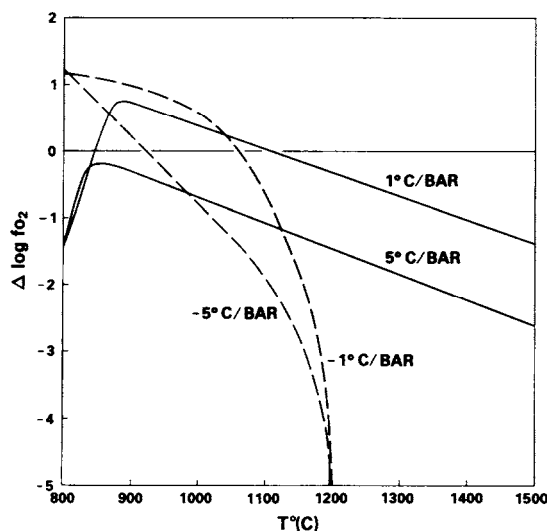
Fig. 7.7.6. The T-Δlog fO$_2$ regime within four hypothetical meteorite parent bodies lying on the graphite surface. Δlog fO$_2$ is the log fO$_2$ of the graphite surface minus log fO$_2$ of IW. Two parent bodies have positive thermal gradients (1°C/bar, 5°C/bar) with a surface temperature of 800° C. The other two bodies have negative thermal gradients ($-$1° C/bar, $-$5° C/bar) and a surface T of 1200°C (figure after Brett and Sato 1984).

was dissolved, the activity of C would have been lowered. The system would lie below this C (metal) surface at equivalent P and T, and would be buffered by the Fe species.

In principle, meteorites lying on the graphite surface could have experienced quite different fO$_2$ regimes and have resided relatively close to one another in the same parent body, separated by a temperature and pressure gradient (Brett and Sato 1984).

7.7.6. SUMMARY

The existing data on chondrite oxidation states and intrinsic O fugacities lend themselves to a variety of interpretations. Such ambiguities notwithstanding, it is worthwhile to present a summary of tentative conclusions based on our current understanding of the data.

1. A variety of oxidation states are exhibited by the chondritic meteorites. Petrologic and chemical data can be used to arrange the major chondrite groups in order of oxidation state; from highest to lowest, this order is: CI > CM > CV > CO > LL > L > H > EL > EH. Many ungrouped chondrites as well as the silicate inclusions in IAB irons lie between H and E chondrites in this sequence.

2. Intrinsic O fugacity measurements on chondrite whole-rock samples display a corresponding ordering of oxidation states. Again, from highest to lowest, this order is generally $CO > LL \simeq L \simeq H > E$. However, this sequence is based on a much smaller number of samples than that deduced from petrologic and chemical data, and may be subject to experimental errors.

3. Relatively unaltered primitive materials that originally equilibrated with the solar-nebular gas and still retain the imprint of nebular processes may preserve information on the O fugacity of nebular gas.

4. Fayalitic olivines coexisting with metallic Fe found primarily in the matrix of primitive, little-metamorphosed chondrites may preserve information on the O fugacity of local nebular gas.

5. Formation of these fayalitic olivines may have occurred at low temperatures (≤ 500 K) in a gas of solar composition or at higher temperatures in a more oxidizing gas. Neither alternative is unambiguously favored by the available experimental, observational and theoretical data. The former alternative may not be kinetically feasible, whereas the latter requires an unspecified mechanism for producing a highly oxidizing region.

6. Several different oxidation-state indicators are present in Ca,Al-rich inclusions in carbonaceous chondrites: e.g., Mo and W depletions relative to other refractory siderophiles of similar volatility; Ti^{3+}/Ti^{4+} ratios in hibonite; depletions of Ba, Ce, U and V. These indicators are consistent with oxidation at high temperatures in the solar nebula.

7. Metamorphosed chondrites and igneous meteorites that were substantially altered by metamorphic reactions, outgassing and igneous processes may preserve information on the oxidation state and size of their parent bodies. If ordinary chondrites underwent some reduction by graphite, we can deduce that they were derived from parent bodies at least 30 to 70 km in diameter.

It is likely that a combination of experimental, observational and theoretical work in some key areas will aid our understanding of nebular and parent-body processes that may have influenced the oxidation state of chondrites. The following studies are particularly important in this regard:

1. Detailed observational studies of the zoning patterns and trace-element contents of individual fayalite-rich olivine grains from primitive, little-metamorphosed chondrites.

2. Intrinsic O-fugacity measurements of individual components (e.g., chondrules and CAIs) and separated phases (e.g., CAI pyroxene and hibonite; matrix olivine grains) from primitive little-metamorphosed chondrites. Such measurements will provide much needed data for calibrating indirect fO_2 estimates and for testing theoretical models.

3. Laboratory studies of the kinetics of FeO incorporation into olivine and low-Ca pyroxene at low temperatures and at the solar (H_2O/H_2) ratio.

4. Theoretical models of the relative rates of gas-solid and solid-solid reactions that are important for the incorporation of FeO into silicates.

5. More detailed theoretical models of nebular radial mixing and thermal evolution.

These and related studies hold great potential to help unravel the physical and chemical conditions prevailing in the solar nebula and early solar system. The most challenging aspect of these studies is in distinguishing nebular effects from parent-body processes.

REFERENCES

Afiattalab, F., and Wasson, J. T. 1980. Composition of the metal phases in ordinary chondrites: Implications regarding classification and metamorphism. *Geochim. Cosmochim. Acta* 44: 431–446.

Agosto, W. N., Hewins, R. H., and Clarke, R. S., Jr. 1980. Allan Hills A77219, the first Antarctic mesosiderite. *Proc. Lunar Planet. Sci. Conf.* 11:1027–1045.

Armstrong, J. T., El Goresy, A., and Wasserburg, G. J. 1985a. Willy: A prize noble Ur-Fremdling—Its history and implications for the formation of Fremdlinge and CAI. *Geochim. Cosmochim. Acta* 49:1001–1022.

Armstrong, J. T., Hutcheon, I. D., and Wasserburg, G. J. 1985b. Ni-Pt-Ge-rich Fremdlinge: Indicators of a turbulent early solar nebula. *Meteoritics* 20:603–604 (abstract).

Basaltic Volcanism Study Project. 1981. *Basaltic Volcanism on the Terrestrial Planets* (New York: Pergamon Press).

Beckett, J. R. 1986. The origin of Ca, Al-rich inclusions from carbonaceous chondrites: An experimental study. Ph.D. thesis, Univ. of Chicago.

Bischoff, A., and Palme, H. 1987. Composition and mineralogy of refractory-metal-rich assemblages from a Ca,Al-rich inclusion in the Allende meteorite. *Geochim. Cosmochim. Acta* 51:2733–2748.

Boynton, W. V. 1984. Cosmochemistry of the rare earth elements: Meteorite studies. In *Rare Earth Element Geochemistry,* ed. P. Henderson (Amsterdam: Elsevier), pp. 63–114.

Brett, R., and Sato, M. 1984. Intrinsic oxygen fugacity measurements on seven chondrites, a pallasite, and a tektite and the redox state of meteorite parent bodies. *Geochim. Cosmochim. Acta* 48:111–120.

Brett, R., Huebner, J. S., and Sato, M. 1977. Measured oxygen fugacities of the Angra dos Reis achondrite as a function of temperature. *Earth Planet. Sci. Lett.* 35:363–368.

Davis, A. M., Tanaka, T., Grossman, L., Lee, T., and Wasserburg, G. J. 1982. Chemical composition of HAL, an isotopically-unusual Allende inclusion. *Geochim. Cosmochim. Acta* 46:1627–1651.

Dodd, R. T. 1974. The metal phase in unequilibrated ordinary chondrites and its implications for calculated accretion temperatures. *Geochim. Cosmochim. Acta* 38:485–494.

El Goresy, A., Nagel, K., and Ramdohr, P. 1978. Fremdlinge and their noble relatives. *Proc. Lunar Sci. Conf.* 9:1279–1303.

Fegley, B., Jr. 1986. A comparison of REE and refractory metal oxidation state indicators for the solar nebula. *Lunar Planet. Sci.* XVII:220–221 (abstract).

Fegley, B., Jr., and Kornacki, A. S. 1984. The geochemical behavior of refractory noble metals and lithophile trace elements in refractory inclusions in carbonaceous chondrites. *Earth Planet. Sci. Lett.* 68:181–197.

Fegley, B., Jr., and Palme, H. 1985. Evidence for oxidizing conditions in the solar nebula from Mo and W depletions in refractory inclusions in carbonaceous chondrites. *Earth Planet. Sci. Lett.* 72:311–326.

Gomes, C. B., and Keil, K. 1980. *Brazilian Stone Meteorites* (Albuquerque: Univ. of New Mexico Press).

Gooley, R. C., and Moore, C. B. 1976. Native metal in diogenite meteorites. *Amer. Mineral.* 61:373–378.

Grossman, J. N., and Wasson, J. T. 1983a. Refractory precursor components of Semarkona chondrules and the fractionation of refractory elements among chondrites. *Geochim. Cosmochim. Acta* 47:759–771.

Grossman, J. N., and Wasson, J. T. 1983b. The compositions of chondrules in unequilibrated chondrites: An evaluation of models for the formation of chondrules and their precursor materials. In *Chondrules and Their Origins*, ed. E. A. King (Houston: Lunar and Planetary Inst.), pp. 88–121.

Harlow, G. E., Delaney, J. S., Nehru, C. E., and Prinz, M. 1982. Metamorphic reactions in mesosiderites: Origin of abundant phosphate and silica. *Geochim. Cosmochim. Acta* 46: 339–348.

Hewins, R. H., and Ulmer, G. C. 1984. Intrinsic oxygen fugacities of diogenites and mesosiderite clasts. *Geochim. Cosmochim. Acta* 48:1555–1560.

Holmes, R. D., and Arculus, R. J. 1982. Metal-silicate redox reactions: Implications for core mantle equilibrium and the oxidation state of the upper mantle. *Lunar Planet. Sci.* XIII:45–46 (abstract).

Hua, X., Adam, J., Palme, H., and El Goresy, A. 1987. Fayalite-rich rims around forsteritic olivines in CAIs and chondrules in carbonaceous chondrites: Types, compositional profiles and constraints of their formation. *Lunar Planet. Sci.* XVIII:443–444 (abstract).

Ihinger, P. D., and Stolper, E. 1986. The color of meteoritic hibonite: An indicator of oxygen fugacity. *Earth Planet. Sci. Lett.* 78:67–79.

JANAF Thermochemical Tables, third ed. 1986. Eds. M. W. Chase, C. A. Davies, J. R. Downey, D. J. Frurip, R. A. McDonald, and A. N. Syverud, *Suppl. 1 to Jour. Phys. Chem. Ref. Data* 14.

Kallemeyn, G. W., and Wasson, J. T. 1985. The compositional classification of chondrites: IV. Ungrouped chondritic meteorites and clasts. *Geochim. Cosmochim. Acta* 49:261–270.

Kozul, J., Ulmer, G. C., and Hewins, R. 1986. Allende inclusions are oxidized! *Eos, Trans. AGU* 67:300 (abstract).

Larimer, J. W. 1968a. Experimental studies on the system Fe-MgO-SiO_2-O_2 and their bearing on the petrology of chondritic meteorites. *Geochim. Cosmochim. Acta* 32:1187–1207.

Larimer, J. W. 1968b. An experimental investigation of oldhamite CaS; and the petrologic significance of oldhamite in meteorites. *Geochim. Cosmochim. Acta* 32:965–982.

Larimer, J. W., and Bartholomay, M. 1979. The role of carbon and oxygen in cosmic gases: Some applications to the chemistry and mineralogy of enstatite chondrites. *Geochim. Cosmochim. Acta* 43:1455–1466.

Larimer, J. W., and Buseck, P. R. 1974. Equilibration temperatures in enstatite chondrites. *Geochim. Cosmochim. Acta* 38:471–477.

Lewis, J. S., and Prinn, R. G. 1980. Kinetic inhibition of CO and N_2 reduction in the solar nebula. *Astrophys. J.* 238:357–364.

Lewis, J. S., Barshay, S. S., and Noyes, B. 1979. Primordial retention of carbon by the terrestrial planets. *Icarus* 37:190–206.

Live, D., Beckett, J. R., Tsay, F.-D., Grossman, L., and Stolper, E. 1986a. Ti^{3+} in meteoritic and synthetic hibonite: A new oxygen barometer. *Lunar Planet. Sci.* XVII:488–489 (abstract).

Live, D., Tsay, F. D., Beckett, J. R., and Stolper, E. 1986b. Determination of oxygen fugacities in the early solar system. *Eos, Trans. AGU* 67:1071 (abstract).

Mason, B. 1979. Chapter B, Cosmochemistry, Part 1. Meteorites. In *Data of Geochemistry*, sixth ed., ed. M. Fleischer, U.S. Geol. Survey Prof. Paper 440-B-1.

McSween, H. Y. 1977a. Petrographic variations among carbonaceous chondrites of the Vigarano type. *Geochim. Cosmochim. Acta* 41:1777–1790. -

McSween, H. Y. 1977b. Carbonaceous chondrites of the Ornans type: A metamorphic sequence. *Geochim. Cosmochim. Acta* 41:477–491.

McSween, H. Y., and Stolper, E. M. 1978. Shergottite meteorites I: Mineralogy and petrography. *Lunar Planet. Sci.* IX:732–734 (abstract).

Mueller, R. F., and Saxena, S. A. 1977. *Chemical Petrology* (New York: Springer-Verlag).

Nagahara, H. 1984. Matrices of type 3 ordinary chondrites—primitive nebular records. *Geochim. Cosmochim. Acta* 48:2581–2595.'

Noonan, A. F., Fredriksson, K., Jarosewich, E., and Brenner, P. 1976. Mineralogy and bulk, chondrule, size-fraction chemistry of the Dhajala, India, chondrite. *Meteoritics* 11:340–343 (abstract).

Olsen, E., and Fredriksson, K. 1966. Phosphates in iron and pallasite meteorites. *Geochim. Cosmochim. Acta* 30:459–470.

Olsen, E., and Fuchs, L. H. 1967. The state of oxidation of some iron meteorites. *Icarus* 6:242–253.

Palme, H., and Fegley, B., Jr. 1987. Formation of FeO-bearing olivines in carbonaceous chondrites by high temperature oxidation in the solar nebula. *Lunar Planet Sci.* XVIII:754–755 (abstract).

Pellas, P., and Storzer, D. 1981. ^{244}Pu fission track thermometry and its application to stony meteorites. *Proc. Roy. Soc. London* A374:253–270.

Prinn, R. G., and Fegley, B., Jr. 1988. Solar nebula chemistry: Origin of planetary, satellite, and cometary volatiles. In *Planetary and Satellite Atmospheres: Origin and Evolution*, eds. S. K. Atreya, J. B. Pollack and M. S. Matthews (Tucson: Univ. of Arizona Press), in press.

Prinz, M., Nehru, C. E., Delaney, J. S., and Weisberg, M. 1983. Silicates in IAB and IIICD irons, winonaites, lodranites, and Brachina: A primitive and modified primitive group. *Lunar Planet. Sci.* XIV:616–617 (abstract).

Rambaldi, E. R., Sears, D. W., and Wasson, J. T. 1980. Si-rich Fe-Ni grains in highly unequilibrated chondrites. *Nature* 287:817–820.

Reid, A. M., and Bunch, T. E. 1975. The nakhlites, part II: Where, when, and how. *Meteoritics* 10:317–324.

Sato, M. 1972. Intrinsic oxygen fugacities of iron-bearing oxide and silicate minerals under low total pressure. *Geol. Soc. Amer. Mem.* 135:289–307.

Sato, M. 1978. A possible role of carbon in characterizing the oxidation state of a planetary interior and originating a metallic core. *Lunar Planet. Sci.* IX:990–992 (abstract).

Sato, M. 1979. The driving mechanism of lunar pyroclastic eruptions inferred from the oxygen fugacity behavior of Apollo 17 orange glass. *Proc. Lunar Planet. Sci. Conf.* 10:311–325.

Scott, E. R. D., Rubin, A. E., Taylor, G. J., and Keil, K. 1984. Matrix in type 3 chondrites— Occurrence, heterogeneity and relationship with chondrules. *Geochim. Cosmochim. Acta* 48:1741–1757.

Scott, E. R. D., Lusby, D., and Keil, K. 1985. Ubiquitous brecciation after metamorphism in equilibrated ordinary chondrites. *Proc. Lunar Planet. Sci. Conf.* 16, *J. Geophys. Res. Suppl.* 90:D137–D148.

Scott, E. R. D., Taylor, G. J., and Keil, K. 1986. Accretion, metamorphism, and brecciation of ordinary chondrites: Evidence from petrologic studies of meteorites from Roosevelt County, New Mexico. *Proc. Lunar Planet. Sci. Conf.* 17, *J. Geophys. Res. Suppl.* 91:E115–E123.

Smith, J. V., and Hervig, R. L. 1979. Shergotty meteorite: Mineralogy, petrography, and minor elements. *Meteoritics* 14:121–142.

Snellenburg, J. W., Nehru, C. E., Caulfield, J. B. D., Zucker, S., and Prinz, M. 1979. Petrology of temperature and oxygen fugacity indicating mineral assemblages in four low grade mesosiderites. *Lunar Planet. Sci.* X:1137–1138 (abstract).

Stolper, E. 1977. Experimental petrology of eucritic meteorites. *Geochim. Cosmochim. Acta* 41:587–611.

Wasson, J. T. 1985. *Meteorites: Their Record of Early Solar-System History* (New York: W. H. Freeman).

Williams, R. J. 1971. Equilibrium temperatures, pressures, and oxygen fugacities of the equilibrated chondrites. *Geochim. Cosmochim. Acta* 35:407–411.

Wood, J. A. 1985. Meteoritic constraints on processes in the solar nebula. In *Protostars & Planets II*, eds. D. C. Black and M. S. Matthews (Tucson: Univ. of Arizona Press), pp. 687–702.

Wood, J. A. 1988. Chondritic meteorites and the solar nebula. *Ann. Rev. Earth Planet. Sci.* 16, in press.